

EFFECTS OF FIBER REINFORCEMENT ARCHITECTURE ON THE HYGROTHERMAL-MECHANICAL PERFORMANCE OF POLYIMIDE MATRIX COMPOSITES FOR AEROPROPULSION APPLICATIONS[†]

E. Eugene Shin¹, John C. Thesken¹, James K. Sutter, Kathy Chuang, John Juhas, Adrienne Veverka, Linda Inghram¹, Demetrios Papadopoulos², Chris Burke³, Dan Scheiman³, Linda McCorkle¹, Ojars Klans

NASA Glenn Research Center, 21000 Brookpark Rd., Cleveland, OH 44135

On-Site Contract via ¹ OAI; ² QSS; ³ U. of Akron

Tel: 216-433-2544, Fax: 216-977-7132, E-mail: E.Eugene.Shin@grc.nasa.gov

and

Jeff Fink, Boeing-Rocketdyne, Canoga Park, CA 91309-7922

C. Arendt, T. Tsotsis, P. Keister, R. Kollmansberger, Boeing, Huntington Beach, CA 92647

Doug Armstrong, Fiber Innovations Inc. (FII), Walpole, MA 02081

Matt Taylor, Integrated Technologies, Inc (Intec), Bothell, WA 98021

Maciej Kumosa, University of Denver, Denver, CO 80210

Brian Rice, Thao Gibson, University of Dayton Research Institute, Dayton, OH 45469

ABSTRACT

A rigid lightweight sandwich support structure, for the combustor chamber of a new generation liquid propellant rocket engine, was designed and fabricated using polymer matrix composite (PMC) facesheet on a Ti honeycomb core. The PMC facesheet consisted of high stiffness carbon fiber, M40JB, and high temperature Polyimides, such as PMR-II-50 and HFPE-II-52. Six different fiber architectures; four harness satin (4HS) woven fabric, uni-tape, woven-uni hybrid, stitched woven fabric, stitched uni-tape and triaxial braided structures have been investigated for optimum stiffness-thickness-weight-hygrothermal performance design criteria for the hygrothermal-mechanical propulsion service exposure conditions including rapid heating up to 200°F/sec, maximum operating temperature of 600°F, internal pressure up to 100psi. One of the specific objectives in this study is to improve composite blistering resistance in z-direction at minimum expense of in-plane mechanical properties.

An extensive property-performance database including dry-wet mechanical properties at various temperatures, thermal-physical properties, such as blistering onset condition was generated for fiber architecture down-selection and design guidelines. Various optimized process methods such as vacuum bag compression molding, solvent assistant resin transfer molding (SaRTM), resin film infusion (RFI) and autoclaving were utilized for PMC panel fabrication depending on the architecture type. In the case of stitched woven fabric architecture, the stitch pattern in terms of stitch density and yarn size was optimized based on both in-plane mechanical properties and blistering performance. Potential reduction of the in-plane properties transverse to the line of stitching was also evaluated. Efforts have been made to correlate the experimental results with theoretical micro-mechanics predictions. Changes in deformation mechanism and failure sequences in terms of fiber architecture will be discussed.

KEY WORDS: Polyimide matrix, PMR-II-50/M40J composites, Fiber architecture, Composite processing, Hygrothermal-mechanical Aeropropulsion performance

INTRODUCTION

[†] This paper is a work of the US Government and is not subject to copyright laws

High temperature PMCs are required to increase thrust to weight ratios for many propulsion applications and graphite fiber polyimide composites are well suited for these applications. A collaborative project between NASA Glenn Research Center and Boeing Rocketdyne focuses on propulsion components that are candidates for *Access to Space* applications (1-5). A second generation PMR (*in situ* polymerization of monomer reactants) polyimide resin (6-10) was considered for these high temperature and high stiffness space propulsion applications, such as face-sheet of sandwich structures.

One of the material-process variables that can modify properties and performance of PMC is the fiber architecture (4-5, 11-15). This increases the flexibility in PMC component design and material selection for various applications, but requires extensive property and performance database. Currently, most graphite fiber polyimide composites are manufactured using 2-dimensional preregs. However, space propulsion components undergo rapid heating and residual moisture can cause composite blistering or delamination in z-direction. Recently, efforts have focused on developing advanced fiber architectures to improve the through-thickness strength; preferably, at minimum expense of in-plane mechanical properties. Therefore, this program extends the use of graphite fiber polyimide composites into the several fiber architectures such as stitching and tri-axial braids. For each fiber architecture type, an optimal composite processing method was selected.

The planned roadmap of this research program is illustrated in Figure 1. The objective of this study is to optimize the hygrothermal-mechanical-structural performance of PMC in terms of fiber architecture while maintaining the benefit of weight reduction and to generate a database for other similar applications.

EXPERIMENTAL

Table I summarizes the overall test matrix in terms of fiber reinforcement architecture types and their mechanical, thermal, and hygrothermal-mechanical properties to be evaluated. The effects of composite thickness were also characterized in terms of in-plane tensile properties as well as hygrothermal-induced blistering performance. Fiber areal weight (FAW) of all architectures was kept constant and all composites were fabricated for a fiber volume fraction (FVF) of ~ 60%. The 4HS fabric was used as the baseline architecture and twelve-ply panels with a cross ply configuration of $[0_b 90_b 90_b 0_b 0_b 90_b]_{1s}$ was the stiffness driven baseline configuration. The lay-up was balanced, symmetric and optimized to reduce the amount of fiber crimping lines so that residual stresses that cause panel warpage would be minimized (16). Similar lay-up sequences were used for other architectures except the tri-axial braided structure and other panels with different thicknesses as specified in Table I.

Materials The PMR resins used were PMR-II-50 for most architecture types and HFPE-II-52 (9) for the stitched uni-tape. The latter was modified with more hygrothermally stable PEPE (4-phenylethynyl-phthalic acid, methyl ester) endcap, Figure 2, and optimized and produced at NASA-GRC for the RFI process. The PMR-II-50 resin solutions were prepared by Maverick Corp., in Blue Ash, OH (4). The carbon fiber selected for this study was M40JB with density of 1.77 g/cm^3 , Young's modulus of 54.7Msi, and strain-to-failure of 1.2%. Fibers in 6k-tow were purchased from Toray Carbon Fibers America, Inc.,

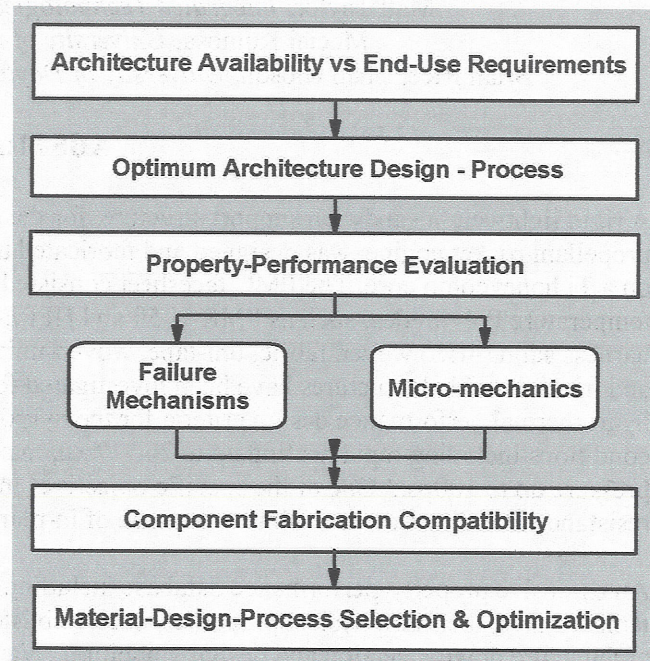


Figure 1 Overall program Plan

Santa Ana, CA. The fibers were woven into a 4HS fabric or a uni-tape (Constructex™) with a FAW of 215 gm/m² or 110 gm/m², respectively, at Sigmatex High Technology Fabrics, Inc., Benicia, CA. or braided at FII. M40J had an epoxy sizing and was used as received.

Table I Overall Test Matrix

TEST TYPE		COMPOSITE PANEL TYPE (PMR-II-50/M40JB): FIBER ARCHITECTURE					
PROPERTIES	CONDITIONS	4HS WOVEN FABRIC	UNI-TAPE CROSS-PLY	UNI-WOVEN HYBRID	TRIAXIAL BRAID	STITCHED	
						UNI-TAPE	4HS WOVEN
Compression (3 repeats)	Dry RT	• 12-ply fabric; [0 _n ,90 _n ,90 _n ,0 _n ,0 _n ,90 _d] _{1s}	• 24-ply uni; [0,90,90,0,90,0,0,0,90,0,90,90,0] _{1s}	• 8-ply fabric + 8-ply uni; [0 _n ,90,0,90,0 _n ,0,90,90] _{1s}			
	Dry T _{max} (600°F) Wet T _{max} (600°F)						
Open Hole Comp/Northrop (3 repeats)	Dry RT	~0.1" TH	~0.1" TH	~0.1" TH			
	Dry T _{max} (600°F) Wet T _{max} (600°F)						
Tension (3 repeats)	Dry RT	• 2-; [0] _{1s} , 0.02" TH • 4-; [0 _n ,90] _{1s} , 0.033" TH • 12-ply fabric	• 4-; [0,90] _{1s} , 0.02" TH • 8-; [0,90,90,0] _{1s} , ~0.035" TH • 24-ply uni	• 8/8 fabric/uni; • 2/4 fabric/uni; [0 _n ,90,0] _{1s} ; ~0.035" TH	• Equivalent to 12-ply fabric, By SaRTM ~0.1" TH	• 24-ply uni; [0,90] _{1s} ; • HFPE-II-52 • By RFI ~0.11" TH	• 12-ply fabric; [0 _n ,90 _n ,90 _n ,0 _n ,0 _n ,90 _d] _{1s} • By SaRTM ~0.11" TH
	Dry T _{max} (600°F)						
	Wet T _{max} (600°F)						
SBS (6 repeats)	Dry RT	• 12-ply fabric	• 24-ply uni	• 8-ply fabric + 8-ply uni			
	Dry T _{max} (600°F) Wet T _{max} (600°F)						
In-plane Shear (Iosipescu) (3 repeats)	Dry RT	• 12-ply fabric	• 24-ply uni	• 8-ply fabric + 8-ply uni			
	Dry T _{max} (600°F) Wet T _{max} (600°F)						
DMA	RT to 500°C	• 6-; [0 _n ,90 _n ,0] _{1s} , 0.052" TH • 8-; [0 _n ,90 _n ,90 _n ,0] _{1s} , 0.065" TH					
TMA (both X & Z)	RT to 500°C						
TGA	RT to 800°C						
Thermal Cond.	RT to T _{max} (600°F)						
Moisture Diff.	RT to 80°F	2, 4, 6, 8, & 12-ply fabric	4, 8 and 24-ply uni	• 8/8 fabric/uni • 2/4 fabric/uni			
Blistering (Fully Saturated)	2"×2" coupon 12"×12" panel						
Hygrothermal Rapid heat-up Cycle (w/ 12"×12" panel), 1 - 200 cycles		Selected Architecture Systems Only					

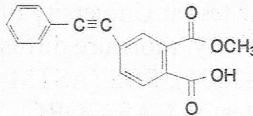
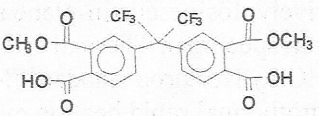

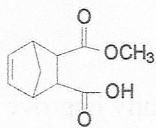
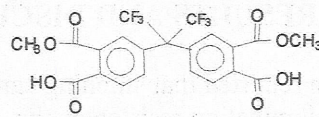
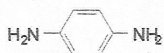
	Endcap	Dimethyl Ester	Diamine	Repeat Unit(n)
Molar Ratio	2	n	n+1	
HFPE	 PEPE	 H FDE	 p-PDA	9
PMR-II-50	 NE	 HFDE	 p-PDA	9

Figure 2 Monomer Chemical Structures of PMR Matrix Resins

Composite Processing and Quality Control For the three 2-D architectures, all composite panels in 12"×12" dimensions were fabricated at NASA-GRC via standard solution prepregging, hand lay-up, B-staging, vacuum bag hot press molding in hydraulic press, and free standing postcure. Preforms and

composite panels of the stitched woven and the tri-axial braid were fabricated at FII using SaRTM process (17). For the stitched uni-tape, stitching and composite fabrication were conducted at Boeing Huntington Beach using RFI process and autoclave molding. Figure 3 shows typical exterior texture of the six different fiber architectures. Detailed fabrication procedures and the optimized cure and postcure cycles used in those processes were reported earlier (5). Composite panels were C-scanned using an ULTRAPAC-AD-500 from Physical Acoustics with 5MHz probe before and after postcure. Void content and FVF of composites were determined by the acid digestion method in ASTM D 3171. Three 3/4"×3/4" sections were collected from various C-scan quality regions. FVF of various composite panels ranged from 57% to 60%. Void contents of most 2-D architecture composites lined up approximately at 1.5% or lower level while 3-D architecture composites had higher void contents, around 4 to 5 %.

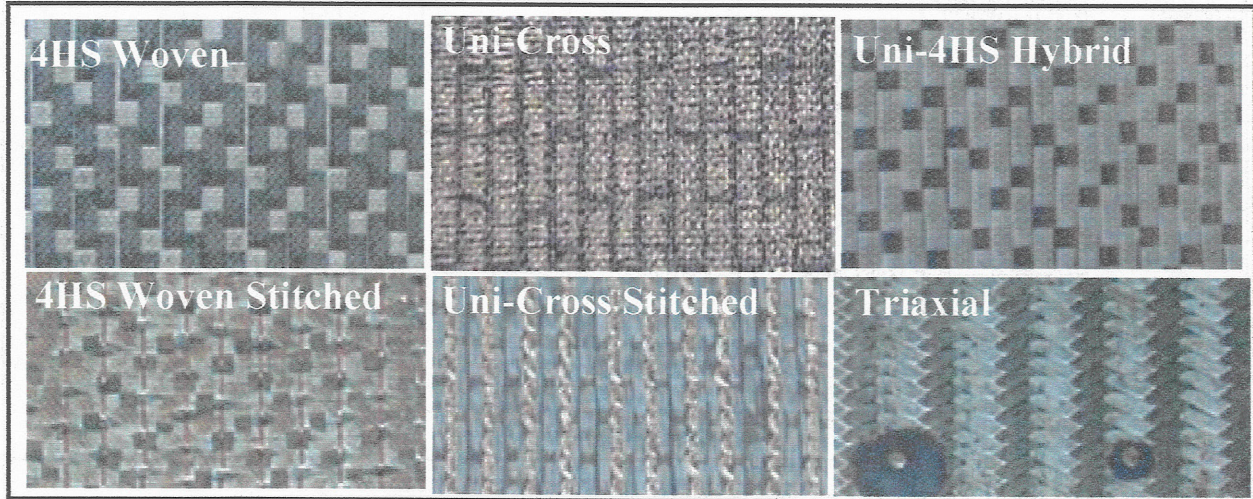


Figure 3 Typical Surface Textures of Various Fiber Architectures

Test Methods Due to considerable quality variation within composite panels test specimens were referenced to their panel's C-scan image. The quality of each specimen is then correlated with mechanical and physical properties. Dry specimens were dried at 120°C (248°F) for 24 hrs in 25 Hg" vacuum and wet samples were conditioned at 71°C (160°F) and 90%RH for 4 days prior to testing. Tension and compression tests were conducted at Intec, following ASTM D3039 using a 9.0" long × 1.5" wide dumbbell shape specimen with a 1.0" wide × 2.8" long gage section and ASTM D3410 with 5.5" long × 0.5" wide specimen, respectively; Iosipescu in-plane shear test at University of Denver based on ASTM D5379 using 20 mm × 90 mm specimen; Thermal conductivity, moisture diffusivity and coupon blistering test at UDRI-AF; and OHC by Northrop standard (NAI-1504), SBS (ASTM D2344), DMA, TMA, panel blistering test, and hygrothermal rapid heating cycle test at NASA-GRC. The test conditions and procedures for various thermal properties, moisture diffusivity, and blistering onset condition were described in detail elsewhere (4, 5, 18).

RESULTS AND DISCUSSION

Stitching Optimization It has been reported that stitching can significantly improve composites through-the-thickness properties, such as delamination resistance, the compression-after-impact strength, and blistering resistance, but at the considerable expense of in-plane mechanical properties (10, 13, 14, 19). The extent of the property modification was strongly dependent on stitching pattern and density as well as fiber type, so it was essential to optimize the stitching parameters for the selected material system. The variables studied for the 4HS Woven Fabric were;

- Stitch penetration density: 4, 6, and 8 stitches per inch
- Stitch-line spacing: 0.12", 0.17", and 0.25"

- Stitching yarn size (S2 glass): thin (150 1/0) vs. thick (150 1/2).

Four different combinations, namely (1) low density: 4 stitches/in-0.25" spacing-thin yarn, (2) medium density 1: 6 stitches/in-0.17" spacing-thin yarn, (3) medium density 2: 6 stitches/in-0.17" spacing-thick yarn, and (4) high density: 8 stitches/in-0.12" spacing-thin yarn, were stitched into each quarter of 15" × 15" 12-ply laminate and RTM-processed at FII. Table II and Figure 4 summarize the results of property and performance evaluation. The two heating rates used in the test were; rate 1: 50°C/min to 250°C ⇒ 5°C/min to 400°C and rate 2: 50°C/min to 400°C. Clearly, blistering was suppressed with the stitching and the 'medium 1' stitching performed best under both heating rates. Note that void content and moisture uptake increased considerably with stitching and they were closely related to each other. The suppression of blistering resulted from two factors; (i) the increased interlaminar strength by stitching and (ii) the increased moisture diffusion path due to higher void content and through stitching channels. They were clearly affected by the stitching density and stitching yarn type in terms of the effective blister dimensions. Earlier extensive studies on the blistering behavior in PMCs were reported elsewhere (4, 18-22) and are also reviewed by Rice and Lee in this ICCM-14 proceedings.

As suggested, the composite in-plane mechanical properties were lowered considerably with stitching. This is discussed further in the later sections. Among the four different stitching densities, both the high and 'medium 1' exhibited better mechanical properties as shown in Figure 4. However, combining the blistering performance and the residual in-plane mechanical properties, the 'medium 1' density was selected for the stitched 4HS woven fiber architecture.

Table II Summary of Blistering Test

Stitch Density	Void Cont. %	Moisture Uptake, %	Blister Onset, °C	
			Rate 1*	Rate 2**
Un-stitched	2.3 ± 0.4	1.47	262	N/A
Low	5.8 ± 0.1	1.74	None	280
Medium 1	4.9 ± 1.2	1.74	None	None
Medium 2; thick yarn	4.6 ± 0.1	1.64	None	310
High	3.6 ± 0.5	1.63	None	N/A

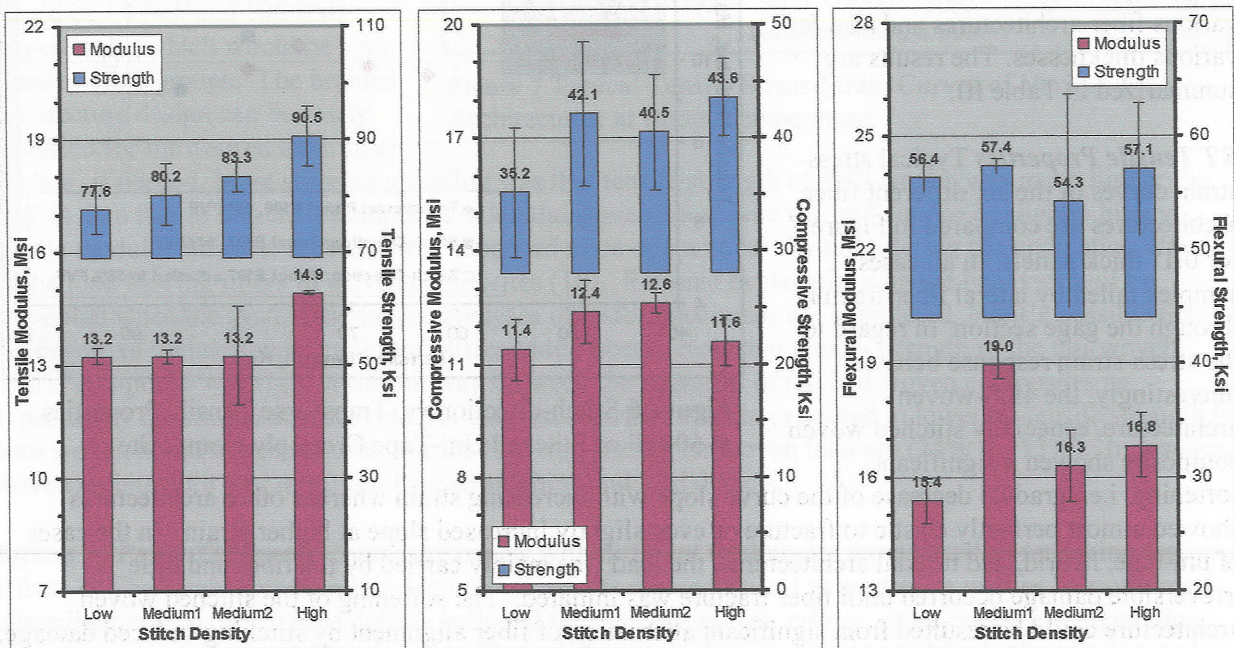


Figure 4 Mechanical Properties for Stitching Optimization of 4HS Woven Composites

Similarly, the stitching of the uni-tape cross-ply architecture was optimized with 40 penetration/in²; 5 stitches/in-1/8" spacing by lock stitch with a fiberglass yarn. In addition, the stitched uni-tape cross-ply architecture was used to study how the unidirectional stitching affected the in-plane mechanical properties in transverse direction. The localized stress field distributions around the voids or the stitch penetrations under the stitch-direction loading might be significantly different from those under the transverse loading. Figure 5 shows the typical cross-section of the stitched uni-tape composite vertical to the stitching direction. Through-thickness stitch penetration lines are visible, but note that voids are mostly distributed around stitch sites along the stitch lines (panel void content, $4.0 \pm 0.5\%$). The effect of loading direction was tested by in-plane tension at 600 °C and plotted in Figure 6. Since the panel tested for the stitch direction had FVF of 54%, its properties were adjusted to FVF of the other panel, 58%, used for transverse tests based on the rule of mixture. The result showed a small change in modulus but about 19% drop in strength. It should be noted that this drop was addition to the strength loss in stitch direction.

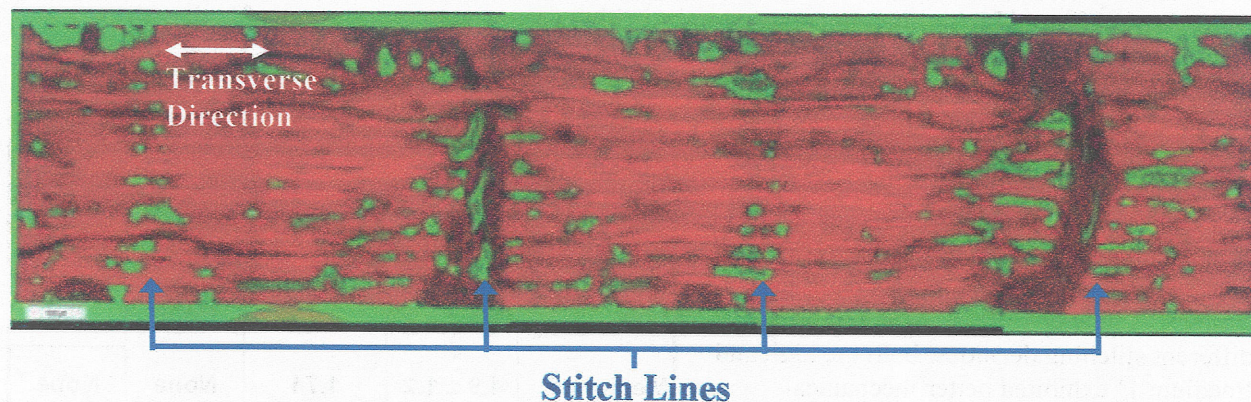


Figure 5 Typical Cross-sectional Optical Micrograph of Stitched Uni-Tape Cross-ply Composite

Mechanical Property vs. Fiber Architecture

To date, both room temperature tensile and compressive properties have been evaluated for various fiber architectures and also for various thicknesses. The results are summarized in Table III.

RT Tensile Properties

Typical stress-strain curves of the six different fiber architectures are compared in Figure 7 for 0.1" thick panels. In all cases, samples failed by lateral fiber fracture through the gage section. In regard to the stress-strain response behavior, interestingly, the 4HS-woven architecture, especially stitched woven composite showed a significant softening, i.e., gradual decrease of the curve slope with increasing strain whereas other architectures showed almost perfectly elastic to fracture or even slightly increased slope at higher strain. In the cases of uni-tape, hybrid, and triaxial architectures, the load was mainly carried by the fiber and little irreversible damage occurred until fiber fracture was initiated. The softening of the stitched woven architecture could be resulted from significant alternation of fiber alignment by stitching-induced damage, such as fiber spreading. Figure 8 shows tensile modulus vs. strength plot for all fiber architectures.

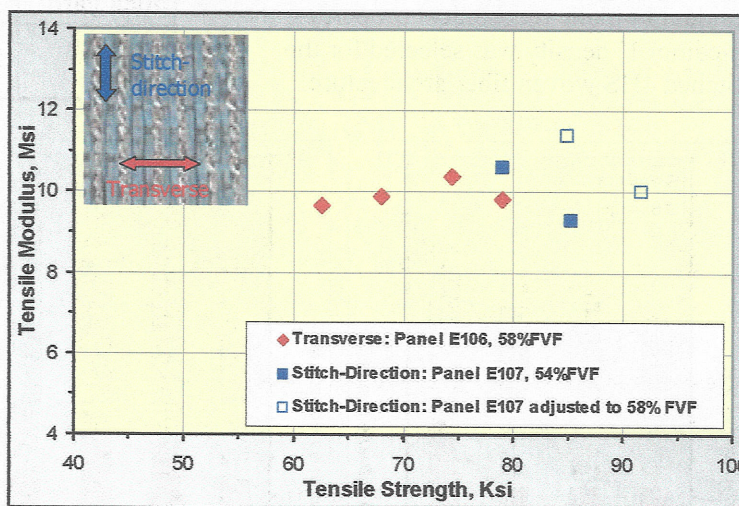
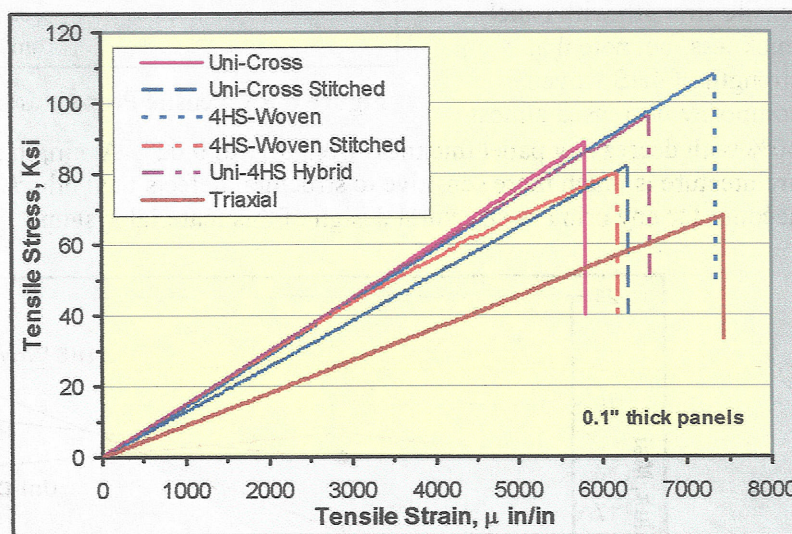


Figure 6 Stitch-direction vs. Transverse Tensile Properties at 600 °F of Stitched Uni-Tape Cross-ply Composite

Table III Summary of Average Tensile and Compressive Properties at Room Temperature

FIBER ARCHITECTURE	Panel Thickness	TENSILE PROPERTIES, RT			COMPRESSIVE PROPERTIES, RT		
		Modulus Msi	Strength Ksi	Strain-to-Failure, $\mu\epsilon$	Modulus Msi	Strength Ksi	Strain-to-Failure, $\mu\epsilon$
4HS WOVEN FABRIC	~0.02"	14.6 \pm 1.3	68.2 \pm 4.2	4765 \pm 659			
	~0.035"	14.9 \pm 0.5	76.5 \pm 1	5180 \pm 452			
	~0.1"	14.6 \pm 0.3	108.3 \pm 5.5	7471 \pm 393	12.7 \pm 0.2	58.5 \pm 3.9	4731 \pm 246
UNI-TAPE CROSS-PLY	~0.02"	13.1 \pm 0.1	92.7 \pm 4.3	6969 \pm 421			
	~0.035"	14.5 \pm 1.1	94.8 \pm 5	6540 \pm 996			
	~0.1"	14.6 \pm 0.5	87.4 \pm 6	5895 \pm 176	11.7 \pm 0.4	56.3 \pm 7.7	4928 \pm 616
UNI-WOVEN HYBRID	~0.035"	16.5 \pm 1.6	89.6 \pm 5.1	5758 \pm 832			
	~0.1"	14.9 \pm 1.8	99.1 \pm 2.5	6227 \pm 1318	11.9 \pm 0.7	43 \pm 2.7	3480 \pm 208
UNI-TAPE STITCHED	~0.1"	13.2 \pm 0.5	75.9 \pm 12	5713 \pm 1037	11.3 \pm 0.4	40.7 \pm 4.7	3413 \pm 605
4HS WOVEN STITCHED	~0.1"	14.6 \pm 1.1	82.2 \pm 7.2	5857 \pm 325	12.9 \pm 0.7	46 \pm 5.5	3598 \pm 603
TRIAXIAL BRAID	~0.1"	9 \pm 0.4	66.8 \pm 3.3	7301 \pm 136	7 \pm 0.4	29.5 \pm 2.2	4334 \pm 96

Except the triaxial architecture, variation of tensile modulus between different architecture types was small, but significant changes were observed in tensile strength. The low modulus and strength of the triaxial architecture was primarily due to lower axial fiber yarn content, ~31%, compared to ~50% in both uni-tape and 4HS woven architectures. If the values were calculated for 50% axial fiber content using the rule of mixture, the tensile modulus and strength would be 14 Msi and 100 Ksi, respectively, which would be very close to other groups. The braided architecture design can be easily modified for the desired axial fiber content, if needed. Most surprising finding was that tensile strength of 4HS woven was much higher (by ~25%) than that of uni-cross composite. Also the woven composite showed similar or slightly higher tensile modulus. Ideally, the trend was supposed to be opposite just by considering the undulation effects of the load-bearing fibers in woven composites (16). Rational explanations on the behavior will be attempted when the systematic failure analyses of tested specimens are completed, but it's possible that the degree of undulation is less in the stiffer M40J fibers. Note that tensile strength of the uni-woven hybrid composite was right at the midway between the strengths of uni and woven composites as expected by the simple mixture rule. As discussed earlier, stitching resulted in lowering tensile strength in both woven and uni architectures, but the loss was greater for woven than uni (24% vs. 13%). In essence, woven architecture was more sensitive to stitching-induced defects.

**Figure 7** Typical Tensile Stress-Strain Curves of Various Fiber Architectures at Room Temperature

Effects of Panel Thickness Composite panels with different thicknesses were tested to determine the effects of fiber architecture-induced structural defects on mechanical properties as well as hygrothermal-blistering performance. These defects included fiber misalignment, crimps, cross-overs, tow separation, fiber-free regions, or local fiber fracture. Three different thicknesses were tested for both uni-cross and 4HS woven architectures and two thicknesses for uni-woven hybrid in tensile loading. The test results are

plotted in Figure 9. By continuum mechanics prediction, the thinner the panels the higher modulus, because of less plane strain effect, (i.e., less thru-the-thickness constraint), and the data showed reasonable trend except the thinnest panels. Tensile modulus of the thinner panels could be more sensitive to the structural defects, especially fiber misalignment. Nevertheless, the change was minimal. Similar explanation can be made for the changes in tensile strength with panel thickness, but note that strength of 4HS woven composite decreased almost

40% with decreasing panel thickness from 0.1" to 0.02". Again, this suggests that the 4HS woven architecture is much more sensitive to structural defects than others. This trend should be taken into account for any primary structural design of this material system.

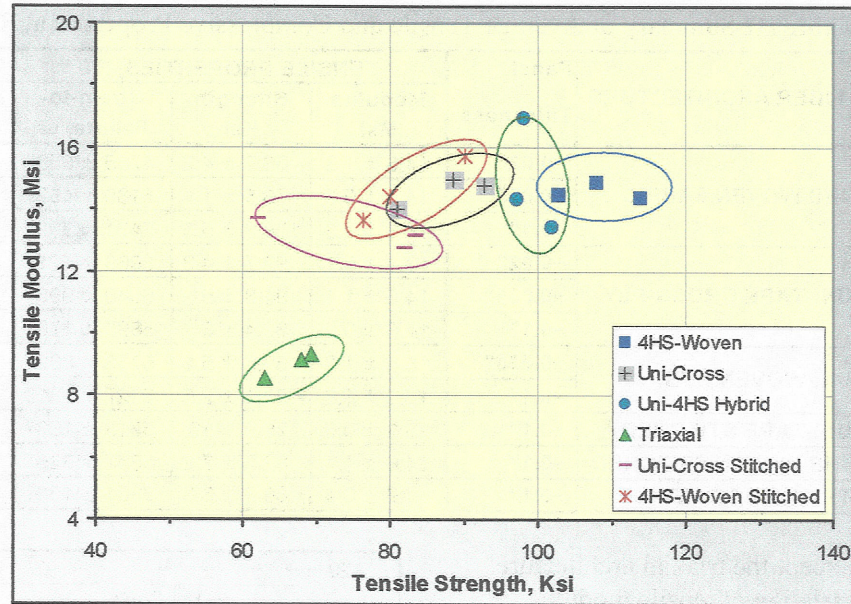


Figure 8 RT Tensile Properties of Various Fiber Architectures

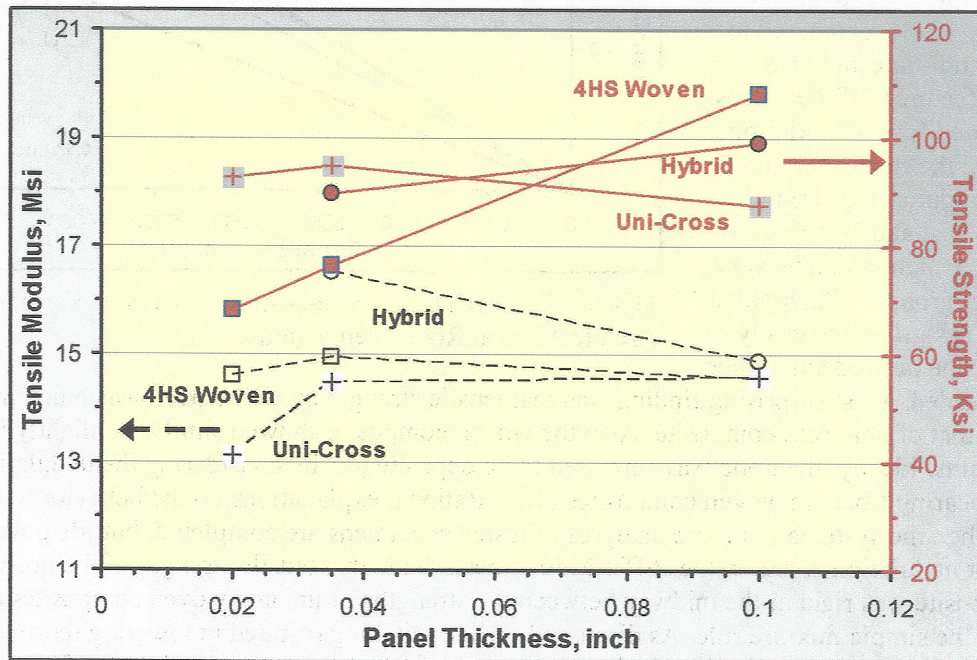


Figure 9 RT Tensile Properties vs. Panel Thickness

RT Compression Properties Unlike tension, the compressive stress-strain curve was similar in shape for all cases that showed slight stress softening by plastic deformation till fracture, Figure 10. This is expected since compressive loading is carried by both fiber axially and matrix transversely or both by shear due to fiber buckling. Thus, compressive properties were significantly lower than tensile properties,

Figure 11. Changes in compressive properties were similar to tensile properties. The low compressive modulus and strength of triaxial architecture was from the same reason as the tensile properties. Similarly, an adjusted value of the compressive modulus and strength by the rule of mixture was 10 Msi and 47 Ksi, respectively. Stitching also lowered compressive strength, but the loss was high for both 4HS woven and uni-cross, 21% vs. 28%.

SUMMARY AND CONCLUSIONS

- Studied six representative fiber architectures, optimized design and process, completed test panel fabrication and test specimen preparation
 - Selected the medium density, 6 stitches/in-0.17" spacing, with thin yarn as the optimum stitching pattern for 4HS woven based on mechanical properties and blistering performance,
 - Transverse property degradation in stitched uni-cross; 15~20% drop in tensile strength in addition to the strength loss in stitch direction
- Completed evaluation of both room temperature tensile and compressive properties as a function of fiber architecture and panel thickness
 - The stitched woven composite showed a significant softening under tensile loading whereas other architectures showed almost perfectly elastic to fracture. This was possibly resulted from significant alternation of fiber alignment by stitching-induced damage, such as fiber spreading
 - Among different fiber architectures, variation of modulus was minimal for both tension and compression, but significant in strength
 - Tensile strength of 4HS woven was ~25% higher than that of uni-cross composite
 - In-plane strength degradation of both stitched panels was about 20 to 30% in both tension and compression

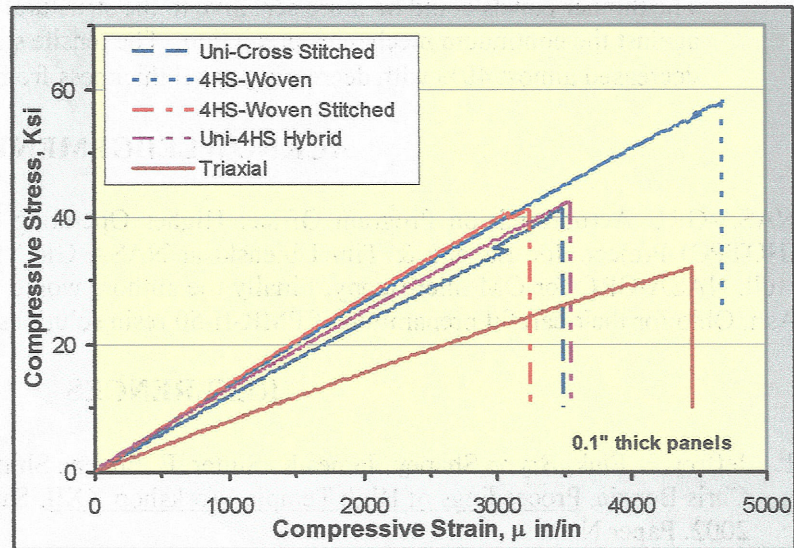


Figure 10 Typical Compressive Stress-Strain Curves of Various Fiber Architectures at Room Temperature

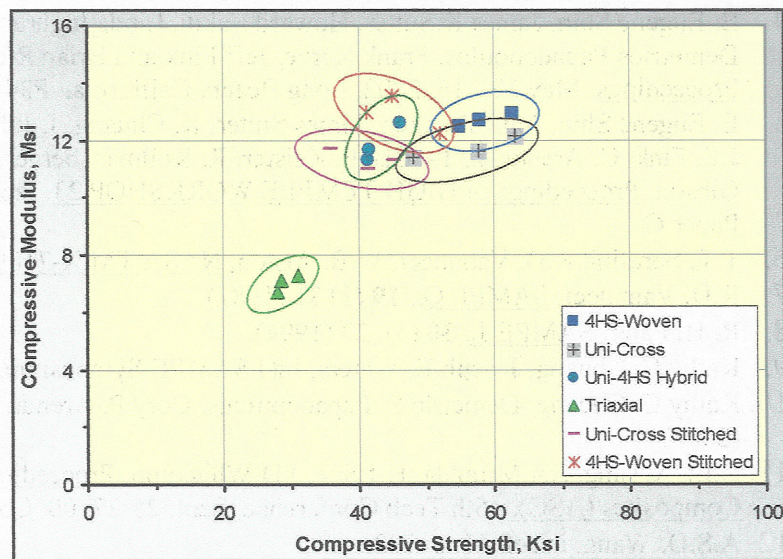


Figure 11 RT Compressive Properties of Various Fiber Architectures

- The thinner panels could be more sensitive to the structural defects, so the properties were lower against the continuum mechanics prediction. The tensile strength of 4HS woven composite decreased almost 40% with decreasing panel thickness from 0.1" to 0.02".

ACKNOWLEDGEMENT

NASA-GRC Aeropropulsion Program Office: Higher Operating Temperature Propulsion Components (HOTPC) Project. Joe Lavelle & Tim Ubienski at NASA GRC for Test specimen preparation. David Hull, NASA-GRC for OM microscopy. Finally the authors would like to thank Maverick Corp., in Blue Ash, Ohio for their careful preparation of PMR-II-50 resin solutions.

REFERENCES

1. Jeffrey E. Fink, Bryon Shapey, James K. Sutter, E. Eugene Shin, John Thesken, Gary Wonacott, and Chris Benzie, Proceedings of High Temple Workshop XXII, Santa Fe, New Mexico, 21-24 January 2002. Paper N.
2. E. Eugene Shin, James K. Sutter, H. Eakin, L. Inghram, L. McCorkle, D. Scheiman, D. Papadopoulos, J. Thesken, and J. Fink, in ref. 1, Paper Y.
3. J. Fink, Boeing Rocket-dyne Propulsion & Power, Private Communication.
4. E. Eugene Shin, James K. Sutter, Howard Eakin, Linda Inghram, Linda McCorkle, Dan Scheiman, Demetrios Papadopoulos, Frank Kerze, Jeff Fink and Brian Rice, SAMPE 2002 Conference Proceedings, May 12 - 16, 2002, Long Beach, California. P341.
5. E. Eugene Shin, John Thesken, James Sutter, K. Chuang, J. Juhas, A. Veverka, L. Inghram, C. Burke, J.E. Fink, C. Arendt, T. Tsotsis, P. Keister, R. Kollmansberger, D. Armstrong, M. Taylor, B. Rice, T. Gibson, Proceedings of HIGH TEMPLE WORKSHOP 23, Jacksonville, FL, 10-13 February 2003, Paper G
6. T.T. Serafini, R.D. Vannucci, W.B. Alston, NASA TM X-71894, April, 1976
7. R.D. Vannucci, SAMPE Q., **19** (1) 31 (1987)
8. R. H. Pater, SAMPE J., **30** (5), 29 (1994).
9. Kathy C. Chuang, Joseph E. Waters, Int'l SAMPE Symposium, 40, 1113 (1995)
10. Kathy C. Chuang, Demetrio S. Papadopoulos, Cory P. Arendt, Int'l SAMPE Symposium, 47, 1175 (2002)
11. C. Li, X. Tang, J.A. Miranda, H.J. Sue, J.D. Whitcomb, Proceedings of the American Society for Composites (ASC), 15th Tech Conference, Sept. 25-27, 00, College Station, TX, pp 780.
12. A.S.D. Wang, in ref. 11, pp772.
13. A.P. Mouritz, K.H. Leong, and I. Herszberg, Composites, Part A, **28A** 979 (1997).
14. K. Dransfield, C. Baillie, Y.W. Mai, Composites Science and Technology, **50**, 305 (1994).
15. Y.Z. Wan, Y.L. Wang, G.X. Cheng, Polymer Composites, v 22, n 1, 111 (2001)
16. S.M. Bishop, Textile Structural Composites, 1989, pp 174-180
17. C. Salemme, D. Armstrong, K. Sargent, Proc. of 31th International SAMPE Tech. Conference, Oct. 26-30, 1999, pp14.
18. B.P. Rice, C.W. Lee, Proc. of 29th International SAMPE Tech. Conference, Oct. 97, pp.675.
19. C.L. Bowman, J.C. Thesken, K. Chuang, and C. Arendt., in ref. 1, paper J.
20. E.E. Shin, C. Dunn, E. Fouch, R.J. Morgan, M. Wilenski, and L.T. Drzal, Proceedings of the ASME Materials Division, **MD-vol. 69-1**, 1995 IMECE, ASME, pp191-200.
21. F. MacDonald, K.C. Chuang, P.B. Stickler, S. Coguill, in ref. 1, paper I.
22. E.E. Shin, R.J. Morgan, J. Zhou, J. Lincoln, R. Jurek and D.B. Curliss, Proceedings of the American Society for Composites (ASC), 12th Tech Conference, Oct. 6-8, 97, Dearborn, MI, pp 1113.